Structural and Functional Characterization of a Macrophage Migration Inhibitory Factor Homologue from the Marine Cyanobacterium Prochlorococcus marinus

Wasiel, Anna A.; Rozeboom, Henriette J.; Hauke, Doreen; Baas, Bert-Jan; Zandvoort, Ellen; Quax, Wim J.; Thunnissen, Andy-Mark W. H.; Poelarends, Gerrit J.

Published in:
Biochemistry

DOI:
10.1021/bi1008276

7572 *Biochemistry* **2010,** *49,* 7572–7581
DOI: 10.1021/bi1008276

BIOCHEMISTRY
including biophysical chemistry & molecular biology
Article

Structural and Functional Characterization of a Macrophage Migration Inhibitory Factor Homologue from the Marine Cyanobacterium *Prochlorococcus marinus*[†,‡]

Anna A. Wasiel,[§] Henriëtte J. Rozeboom,[∥] Doreen Hauke,[§] Bert-Jan Baas,[§] Ellen Zandvoort,[§] Wim J. Quax,[§] Andy-Mark W. H. Thunnissen,*[,∥] and Gerrit J. Poelarends*[,§]

[§]*Department of Pharmaceutical Biology, Groningen Research Institute of Pharmacy, University of Groningen, Antonius Deusinglaan 1, 9713 AV Groningen, The Netherlands, and* [∥]*Laboratory of Biophysical Chemistry, Groningen Biomolecular Sciences and Biotechnology Institute, University of Groningen, Nijenborgh 4, 9747 AG Groningen, The Netherlands*

Received May 25, 2010; Revised Manuscript Received July 1, 2010

ABSTRACT: Macrophage migration inhibitory factor (MIF) is a multifunctional mammalian cytokine, which exhibits tautomerase and oxidoreductase activity. MIF homologues with pairwise sequence identities to human MIF ranging from 31% to 41% have been detected in various cyanobacteria. The gene encoding the MIF homologue from the marine cyanobacterium *Prochlorococcus marinus* strain MIT9313 has been cloned and the corresponding protein (PmMIF) overproduced, purified, and subjected to functional and structural characterization. Kinetic and ^{1}H NMR spectroscopic studies show that PmMIF tautomerizes phenylenolpyruvate and (*p*-hydroxyphenyl)enolpyruvate at low levels. The N-terminal proline of PmMIF is critical for these reactions because the P1A mutant has strongly reduced tautomerase activities. PmMIF shows high structural homology with mammalian MIFs as revealed by a crystal structure of PmMIF at 1.63 Å resolution. MIF contains a Cys-X-X-Cys motif that mediates oxidoreductase activity, which is lacking from PmMIF. Engineering of the motif into PmMIF did not result in oxidoreductase activity but increased the tautomerase activity 8-fold. The shared tautomerase activities and the conservation of the $\beta-\alpha-\beta$ structural fold and key functional groups suggest that eukaryotic MIFs and cyanobacterial PmMIF are related by divergent evolution from a common ancestor. While several MIF homologues have been identified in eukaryotic parasites, where they are thought to play a role in modulating the host immune response, PmMIF is the first nonparasitic, bacterial MIF-like protein characterized in detail. This work sets the stage for future studies which could address the question whether a MIF-like protein from a free-living bacterium possesses immunostimulatory features similar to those of mammalian MIFs and MIF-like proteins found in parasitic nematodes and protozoa.

Macrophage migration inhibitory factor (MIF)[1] was one of the first cytokines to be discovered. It was first identified in mammals as a T-lymphocyte-associated activity released at the site of an infection, where it causes macrophages to concentrate and carry out antigen processing and phagocytosis (*1*, *2*). Since its initial discovery, MIF has been implicated in a number of infectious, inflammatory, and immune responses. MIF is involved in the activation of macrophages, neutrophils, and T-cells and may play a role in conditions such as sepsis, adult respiratory distress syndrome, asthma, bowel disease, rheumatoid arthritis, certain types of cancer and diabetes, and atherosclerosis (*3*−*9*). It is also a unique counterregulator of the immunosuppressive and antiinflammatory activities of glucocorticoids (*10*) and suppresses activation-induced p53-dependent apoptosis (*3*, *5*). Although a classic cytokine receptor has not yet been identified for MIF, it has been proposed that MIF activates cells by binding to the cell surface receptor CD74 (*11*, *12*), which leads to the recruitment and activation of additional signaling proteins, including CD44 and the chemokine receptors CXCR2 and CXCR4 (*12*−*15*).

MIF is notable among cytokines in having two enzymatic activities. MIF functions as an efficient tautomerase, converting phenylenolpyruvate (**1**) to phenylpyruvate (**2**) and (*p*-hydroxyphenyl)enolpyruvate (**3**) to (*p*-hydroxyphenyl)pyruvate (**4**) (Scheme 1) (*16*−*20*). These tautomerase activities and the crystal structure of MIF (*21*, *22*) firmly link this cytokine to the tautomerase superfamily, a group of structurally homologous proteins that are characterized by a conserved catalytic amino-terminal proline embedded within a $\beta-\alpha-\beta$ structural fold (*23*, *24*).[2] Indeed, the tautomerase activities of MIF depend on its Pro-1 residue, which

[†]This research was financially supported by VIDI Grant 700.56.421 (to G.J.P.) from the Division of Chemical Sciences of The Netherlands Organisation for Scientific Research (NWO-CW).

[‡]The coordinates and structure factors have been deposited in the Protein Data Bank (PDB entry 2xcz).

*To whom correspondence should be addressed: G.J.P. (tel, +31-50-3633354; fax, +31-50-3633000; e-mail, g.j.poelarends@rug.nl) or A.-M. W.H.T. (tel, +31-50-3634380; fax, +31-50-3634800; e-mail, a.m.w.h.thunnissen@rug.nl).

[1]Abbreviations: Ap, ampicillin; ESI-MS, electrospray ionization mass spectrometry; HED, 2-hydroxyethyl disulfide; LB, Luria−Bertani; MIF, macrophage migration inhibitory factor; PmMIF, MIF homologue from *Prochlorococcus marinus*; PyMIF, MIF homologue from *Plasmodium yoelii*; NMR, nuclear magnetic resonance; SDS−PAGE, sodium dodecyl sulfate−polyacrylamide gel electrophoresis.

[2]MIF is the title enzyme of one of the five families in the tautomerase superfamily. The other four families are represented by the bacterial enzymes 4-oxalocrotonate tautomerase (4-OT) and 5-(carboxymethyl)-2-hydroxymuconate isomerase (CHMI), found in catabolic pathways for aromatic compounds, and *cis*-3-chloroacrylic acid dehalogenase (*cis*-CaaD) and malonate semialdehyde decarboxylase (MSAD), found in a catabolic pathway for 1,3-dichloropropene (*24*).

 Published on Web 07/16/2010

Scheme 1: Tautomerization Reactions Catalyzed by MIF and PmMIF

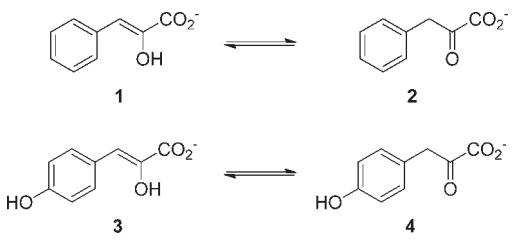

functions as the catalytic base (*20*). It has also been reported that MIF exhibits low-level oxidoreductase activity, reducing small molecule and protein disulfides, which appears to be associated with a thioredoxin-like Cys-X-X-Cys motif (*25*, *26*). It is not yet clear how and if these catalytic activities are related to any of the immunological or inflammatory activities of MIF.

Intriguingly, several eukaryotic parasites have been reported to produce MIF-like proteins that show remarkable functional and structural similarities to mammalian MIFs (*27*−*34*). These include human parasites such as the nematodes *Brugia malayi* and *Ancylostoma ceylonicum* and the protozoa *Leishmania major* and *Plasmodium falciparum*. The question has been raised whether these MIF homologues function as virulence factors and play a role in the parasite−host interaction (*34*, *35*).

In this study, we screened the prokaryotic genomes available in the NCBI database for MIF-like proteins with the aim to identify new MIF family members and provide further insight into the evolutionary history of MIF. We report the identification of a large group of cyanobacterial proteins that share significant sequence identity with mammalian MIFs. The gene encoding the MIF homologue from the marine cyanobacterium *Prochlorococcus marinus* strain MIT9313 has been cloned and the corresponding protein (designated PmMIF) overproduced, purified, and subjected to kinetic, mutational, and structural characterization. The results show that PmMIF is an active tautomerase that shares mechanistic and structural similarities with mammalian MIFs. These observations suggest that cyanobacterial PmMIF and mammalian MIFs are related by divergent evolution and invite speculation about the intrinsic physiological function of MIF-like proteins in marine cyanobacteria. With PmMIF being the first nonparasitic, prokaryotic MIF-like protein characterized in detail, this work sets the stage for future studies that could address the intriguing question whether a MIF-like protein from a free-living bacterium may possess immunostimulatory features similar to those of mammalian MIFs and MIF-like proteins found in parasitic nematodes and protozoa.

EXPERIMENTAL PROCEDURES

Materials. 3-Bromopyruvate, phenylpyruvate, and (*p*-hydroxyphenyl)pyruvate were purchased from Sigma-Aldrich Chemical Co. (St. Louis, MO). Ingredients for media and buffers were obtained from Merck (Darmstadt, Germany) or Duchefa Biochemie (Haarlem, The Netherlands). Molecular biology reagents and protein molecular weight standards were obtained from F. Hoffmann-LaRoche, Ltd. (Basel, Switzerland), Invitrogen Corp. (Carlsbad, CA), Finnzymes (Espoo, Finland), Promega Corp. (Madison, WI), or New England Biolabs (Ipswich, MA). PCR purification, gel extraction, and Miniprep kits were provided by Qiagen (Venlo, The Netherlands) or Macherey-Nagel (Düren, Germany). Prepacked PD-10 Sephadex G-25 columns were purchased from GE Healthcare Bio-Sciences AB (Uppsala, Sweden). Ni-NTA Sepharose or agarose was obtained from Qiagen. Oligonucleotides for DNA amplification were synthesized by Operon Biotechnologies (Cologne, Germany).

General Methods. BLAST searches of the National Center for Biotechnology Information (NCBI) databases were performed using the human MIF amino acid sequence as the query sequence. Amino acid sequences were aligned using a version of the CLUSTALW multiple-sequence alignment routines available in the computational tools at the EMBL-EBI Web site. Techniques for restriction enzyme digestions, ligation, transformation, and other standard molecular biology manipulations were based on methods described elsewhere (*36*) or as suggested by the manufacturer. The PCR was carried out in a DNA thermal cycler (model GS-1) obtained from Biolegio (Nijmegen, The Netherlands). DNA sequencing was performed by ServiceXS (Leiden, The Netherlands) or Macrogen (Seoul, Korea). Protein was analyzed by sodium dodecyl sulfate−polyacrylamide gel electrophoresis (SDS−PAGE) on gels containing 10% polyacrylamide. The gels were stained with Coomassie brilliant blue. Protein concentrations were determined by the method of Waddell (*37*). Kinetic data were obtained on a V-650 spectrophotometer from Jasco (IJsselstein, The Netherlands). The kinetic data were fitted by nonlinear regression data analysis using the Grafit program (Erithacus, Software Ltd., Horley, U.K.) obtained from Sigma Chemical Co. ^{1}H NMR spectra were recorded on a Varian Inova 500 (500 MHz) spectrometer using a pulse sequence for selective presaturation of the water signal. Chemical shifts for protons are reported in parts per million scale (δ scale) downfield from tetramethylsilane and are referenced to protium (H_2O: $\delta = 4.67$). The masses of PmMIF and MIF were determined using an LCQ electrospray mass spectrometer (Applied Biosystems, Foster City, CA), housed in the Mass Spectrometry Facility Core in the Department of Pharmacy at the University of Groningen.

Construction of Expression Vectors for the Production of PmMIF and MIF. The PmMIF gene was amplified from genomic DNA of *P. marinus* strain MIT9313 (*38*) by PCR. Genomic DNA of strain MIT9313 was kindly provided by Dr. S. W. Chisholm (Massachusetts Institute of Technology, Cambridge, MA). The forward primer 5′-CAG CGA **CAT ATG** CCC TTG ATC AAC-3′ contains a *Nde*I restriction site (in bold) followed by 12 bases corresponding to the coding sequence of the PmMIF gene. Two different reverse primers were used. To clone the PmMIF gene in frame with the sequence that codes for the polyhistidine region of the expression vector pET20b(+), the reverse primer 5′-GCA CTG **CTC GAG** ACC GAA GGT ACT TCC-3′, which contains a *Xho*I restriction site (in bold), was used. To clone the gene without fusion tag, the reverse primer 5′-CTG AT**G GAT CC**T CAA CCG AAG GTA CT-3′, which contains a *Bam*HI restriction site (in bold), was used. The MIF gene was PCR-amplified from plasmid pET11b(MIF) (*20*). The forward primer 5′-CAG CGA **CAT ATG** CCT ATG TTC ATC-3′ contains a *Nde*I restriction site (in bold) followed by 12 bases corresponding to the coding sequence of the MIF gene. To clone the MIF gene in frame with the sequence that codes for the polyhistidine region of the expression vector pET20b(+), the reverse primer 5′-CTG ATG GAT **CTC GAG** AGC GAA GGT GGA ACC-3′, which contains a *Xho*I restriction site (in bold), was used.

Amplification mixtures contained the two appropriate synthetic primers, deoxynucleotide triphosphates, template DNA, Phusion DNA polymerase, and Phusion High-Fidelity buffer. The resulting PCR products and the pET20b(+) vector (Novagen)

were digested with the appropriate restriction enzymes, purified, and ligated using T4 DNA ligase. An aliquot of each ligation mixture was transformed into competent *Escherichia coli* DH10B or XL-1 Blue cells. Transformants were selected at 37 °C on LB/Ap plates. Plasmid DNA was isolated from several colonies and analyzed by restriction analysis for the presence of the insert. For each expression vector, the cloned gene was sequenced to verify that no mutations had been introduced during the amplification of the gene. The newly constructed expression vectors were named pET20b(PmMIF-His), pET20b(PmMIF), and pET20b-(MIF-His).

Construction of the PmMIF and MIF Mutants. Mutants of PmMIF and MIF were generated by the overlap extension PCR method (*39*) using plasmid pET20b(PmMIF-His) or pET20b-(MIF-His), respectively, as the template. The final PCR products were gel-purified, digested with *Nde*I and *Xho*I restriction enzymes, and ligated in frame with both the initiation ATG start codon and the sequence that codes for the polyhistidine region of the expression vector pET20b(+). All mutant genes were completely sequenced (with overlapping reads) to verify that only the intended mutation had been introduced.

Expression and Purification of His-Tagged PmMIF and MIF Proteins. The PmMIF and MIF proteins, either wild type or mutant, were produced in *E. coli* BL21(DE3) using the pET20b(+) expression system. Fresh BL21(DE3) cells containing the appropriate expression plasmid were collected from a LB/Ap plate using a sterile loop and used to inoculate LB/Ap medium (10 mL). After growth for 16 h at 37 °C, this culture was used to inoculate fresh LB/Ap medium (1 L) in a 5 L Erlenmeyer flask. Cultures were grown for 16−18 h at 37 °C with vigorous shaking. Cells were harvested by centrifugation (6000*g*, 15 min) and stored at −20 °C until further use.

In a typical purification experiment, cells of a 1 L culture were thawed and suspended in lysis buffer (10 mL, 50 mM NaH_2PO_4, 300 mM NaCl, 10 mM imidazole, pH 8.0). Cells were disrupted by sonication for 6 × 1 min (with 4−6 min rest in between each cycle) at a 60 W output, after which unbroken cells and debris were removed by centrifugation (10000*g*, 45 min). The supernatant was filtered through a 0.45 μM pore diameter filter and incubated with Ni-NTA (1 mL slurry in a small column at 4 °C for ≥18 h), which had previously been equilibrated with lysis buffer. The nonbound proteins were eluted from the column by gravity flow. The column was first washed with lysis buffer (20 mL) and then with buffer A (50 mM NaH_2PO_4, 300 mM NaCl, 20 mM imidazole, pH 8.0; 20 mL). Retained proteins were eluted with buffer B (50 mM NaH_2PO_4, 300 mM NaCl, 250 mM imidazole, pH 8.0; 3 mL). Fractions (~0.5 mL) were analyzed by SDS−PAGE on gels containing acrylamide (10%), and those that contained purified MIF or PmMIF protein were combined, and the buffer was exchanged against 20 mM phosphate buffer (pH 7.3) using a prepacked PD-10 Sephadex G-25 gel filtration column. The purified protein was stored at +4 °C or −80 °C until further use.

Expression and Purification of Native PmMIF. In order to obtain purified native PmMIF without a hexahistidine tag, an alternative purification protocol was developed that used disposable hand-packed columns. Typically, in this protocol, cells from 1 L of culture were suspended in ~10 mL of 10 mM Na_2HPO_4 buffer, pH 8.0 (buffer A), sonicated, and centrifuged as described above. Subsequently, the supernatant was loaded onto a DEAE-Sepharose column (10 × 1.0 cm filled with ~8 mL of resin) that had been previously equilibrated with buffer A. The column was first washed with buffer A (16 mL), and then the protein was eluted by gravity flow using buffer A containing 0.5 M NaCl (8 mL). Fractions (~1 mL) were collected, and PmMIF was identified by SDS−PAGE. The appropriate fractions were pooled and made 1.6 M in $(NH_4)_2SO_4$. After being stirred for 2 h at 4 °C, the precipitate was removed by centrifugation (20 min at 20000*g*), and the supernatant was filtered and loaded onto a phenyl-Sepharose column (10 × 1.0 cm filled with ~8 mL of resin) that had been previously equilibrated with buffer A containing 1.6 M $(NH_4)_2SO_4$. The column was first washed with the loading buffer (16 mL), and then the protein was eluted by gravity flow using buffer A (8 mL). Fractions (~1 mL) were collected and analyzed as described above, and those that contained purified PmMIF protein were combined, and the buffer was exchanged against 20 mM phosphate buffer (pH 7.3) using a prepacked PD-10 Sephadex G-25 gel filtration column. The purified protein was stored at +4 °C or −80 °C until further use. A typical yield is ~50 mg of protein purified to near homogeneity per liter of culture.

Enzymatic Assays. The ketonization of phenylenolpyruvate (**1**) or (*p*-hydroxyphenyl)enolpyruvate (**3**) by MIF, PmMIF, and the PmMIF mutants was monitored by following the depletion of the enol isomer at 255 nm (**1**, ε = 6615 M^{-1} cm^{-1}; **3**, ε = 4423 M^{-1} cm^{-1}) in 20 mM NaH_2PO_4 buffer, pH 6.5, at 22 °C. By monitoring the ketonization of the two substrates at 255 nm, rather than at the reported λ_{max} values for **1** and **3** (288 and 292 nm, respectively) (*20*, *40*), it was possible to use higher substrate concentrations and achieve saturation due to the lower ε values at this wavelength. An appropriate aliquot of each enzyme was diluted into 50 mL of buffer and incubated for at least 30 min at 22 °C. This incubation period results in more reproducible kinetic data. Subsequently, 1 mL aliquots were transferred to a cuvette, and the assay was initiated by the addition of a small quantity (1−10 μL) of either **1** or **3** from a stock solution. Stock solutions (300 mM) of **1** and **3** were initially generated by dissolving the appropriate amount of phenylpyruvic acid or (*p*-hydroxyphenyl)pyruvic acid in ethanol and diluted (with ethanol) to generate 100 and 25 mM solutions. The crystalline free acid of phenylpyruvic acid or (*p*-hydroxyphenyl)pyruvic acid is exclusively the enol form. In general, the concentrations of **1** and **3** used in the assays ranged from 0 to 800 μM. At all substrate concentrations, the nonenzymatic rate was subtracted from the enzymatic rate of ketonization.

^{1}H NMR Spectroscopic Analysis of the Reaction of PmMIF with (p-Hydroxyphenyl)enolpyruvate (*3*). A series of ^{1}H NMR spectra monitoring the PmMIF-catalyzed ketonization of **3** were recorded using the following conditions. An amount of **3** (9 mg, 50 μmol) was dissolved in 2 mL of 50 mM acetate buffer, pH 6.2. An aliquot of this solution (484 μL) was added to an NMR tube containing D_2O (50 μL) and PmMIF (116 μL from a 4.3 mg/mL stock in 20 mM Na_2HPO_4 buffer, pH 7.3). The control sample (for analyzing the nonenzymatic reaction) was prepared in the same way, but now the NMR tube contained 116 μL of 20 mM Na_2HPO_4 buffer, pH 7.3, instead of 116 μL of PmMIF. The first ^{1}H NMR spectrum was recorded immediately after mixing the sample and then after 5, 10, 15, 30, and 60 min.

^{1}H NMR (500 MHz, 50 mM acetate/D_2O buffer, pH 6.2) of (*p*-hydroxyphenyl)pyruvate: enol form, δ = 6.23 (s, H), 6.81 (d, J = 8.7 Hz, 2H), 7.56 (d, J = 8.7 Hz, 2H); keto form, δ = 3.90 (s, 2H), 6.78 (d, J = 8.5 Hz, 2H), 7.03 (d, J = 8.4 Hz, 2H).

Irreversible Inhibition of PmMIF and MIF with 3-Bromopyruvate. In these experiments, MIF and PmMIF were

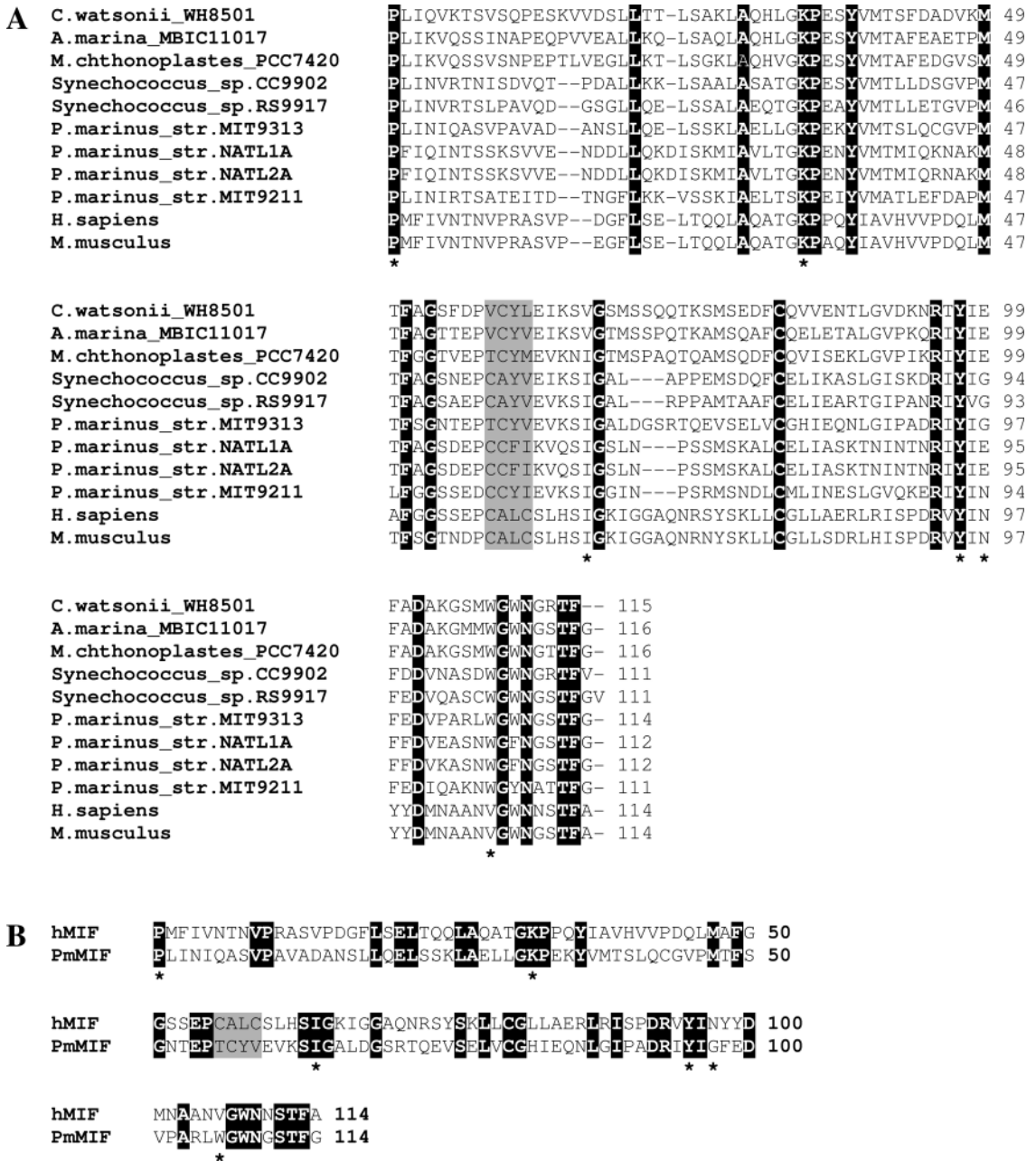

FIGURE 1: MIF-like proteins in cyanobacteria. (A) Amino acid sequence alignment of selected cyanobacterial MIF-like proteins along with human and mouse MIF proteins. The NCBI reference sequences for the selected proteins are as follows: *Crocosphaera watsonii* WH8501, ZP_00514858.1; *Acaryochloris marina* MBIC11017, YP_001515361.1; *Microcoleus chthonoplastes* PCC7420, ZP_05029084.1; *Synechococcus* sp. CC9902, YP_377476.1; *Synechococcus* sp. RS9917, ZP_01079716.1; *P. marinus* strain MIT9313, NP_894336.1; *P. marinus* strain NATL1A, YP_001015373.1; *P. marinus* strain NATL2A, YP_291908.1; *P. marinus* strain MIT9211, YP_001551039.1. (B) Amino acid sequence alignment of the MIF-like protein from *P. marinus* strain MIT9313 (PmMIF) and human MIF (hMIF). Identical residues are shaded in black. The position of the Cys-X-X-Cys motif in the alignments is shaded in gray. The six active site residues that interact with the substrate in the structure of the human MIF−substrate complex (*48*) are indicated by an asterisk.

treated with 3-bromopyruvate in separate incubation mixtures as follows. Each sample contained ~2 mg of enzyme and a sufficient quantity of 100 mM NaH_2PO_4 buffer (pH 7.3) to give a final volume of 1 mL. Each sample was treated with 3-bromopyruvate (10 mM final concentration) and incubated at 22 °C for 1 h. In separate control experiments, the same quantity of MIF or PmMIF was incubated without inhibitor under otherwise identical conditions. Subsequently, the four samples were treated with $NaBH_4$ (25 mM) and loaded onto separate PD-10 Sephadex G-25 gel filtration columns, which had previously been equilibrated with 20 mM NaH_2PO_4 buffer (pH 7.3). The proteins were eluted by gravity flow using the same buffer. Fractions (0.5 mL) were analyzed for the presence of protein by UV absorbance at 215 nm. The appropriate fractions containing the purified proteins were combined and assayed for residual activity and analyzed by ESI-MS.

Crystal Growth and Structure Determination. Purified PmMIF was concentrated to 11 mg/mL in buffer (10 mM Tris-HCl, pH 7.3). The protein was subjected to crystallization trials against 384 commercially available crystallization conditions using the hanging drop vapor diffusion technique. Initial conditions were identified with the Crystal Screen Cryo crystallization kit (Hampton Research) at 293 K. Optimization resulted in the growth of large crystals, obtained from hanging drops with

36−42% PEG300, 0.1 M HEPES, pH 7.5, and 0.2 M NaCl. X-ray diffraction data to 1.63 Å resolution were collected from a single cryocooled crystal mounted on an in-house Bruker AXS rotating anode X-ray generator equipped with a DIP2030 image plate. The crystal belongs to the space group $P6_3$ with cell dimensions $a = b = 52.5$ Å and $c = 64.0$ Å. Data were processed using the program iMosflm (*41*) and programs from the CCP4 suite (Collaborative Computational Project, Number 4, 1994). Phases were obtained by molecular replacement using the program Phaser (*42*). The coordinates of human glycosylation-inhibiting factor (PDB accession code 1GIF) and three macrophage migration inhibitory factor orthologues (1UIZ, 1FIM, and 1GCZ), which all have sequence identities with PmMIF of ~34%, were used to construct a composite search model. The PmMIF structure was built using the programs ArpWarp (*43*) and Coot (*44*), and refined at 1.63 Å resolution using Refmac5 (*45*). Water molecules were placed automatically in $F_o - F_c$ difference Fourier maps at a 3σ cutoff level and validated to ensure correct coordination geometries using Coot. In addition, a diethylene glycol molecule was added to the model based on electron density near Pro-1 in $2F_o - F_c$ and $F_o - F_c$ difference Fourier maps. The last two residues from the PmMIF molecule and the C-terminal His tag were not visible in the electron density and therefore not included in the final model. Relevant statistics of the data collection and model refinement are given in Table 2. The stereochemical quality of the model was assessed with MolProbity (*46*). Figures were prepared with PyMOL (http://www.pymol.org).

Crystallographic Binding Studies. Cocrystallization experiments were performed to bind phenylpyruvate and (*p*-hydroxyphenyl)pyruvate. The drops contained 5 mM of the substrates. Well-diffracting crystals were obtained at similar conditions as before, but the derived electron density revealed no changes in the active site (the same density consistent with a bound poly- or diethylene glycol was present).

RESULTS

Identification of Cyanobacterial MIF Homologues. A BLAST search with the amino acid sequence of human MIF as the query was performed in the NCBI microbial databases containing finished and unfinished genome sequences. This search yielded bacterial proteins that shared significant sequence identity with human MIF, including various sequences from *Synechococcus*, *Prochlorococcus*, and other cyanobacteria. Interestingly, the top 15 hits were sequences from cyanobacteria only. Pairwise identities between human MIF and these identified cyanobacterial MIF homologues range from 31% to 41% (Figure 1A).

The MIF homologue from the marine cyanobacterium *P. marinus* strain MIT9313, designated PmMIF, is annotated as a ATLS1-like light-inducible protein. The genomic context of the gene encoding PmMIF does not provide any clues about the biological function of this protein in *P. marinus* (*38*). The mature PmMIF protein is predicted to be 114 amino acids in length, assuming excision of the initiating methionine residue. The relationship between PmMIF and the MIF family is readily detected by sequence similarity searches. The results of a conserved domain search (CD search) predict the presence of a MIF-like domain in PmMIF. The results of a PSI-BLAST search (with the amino acid sequence of PmMIF as the query) further support this prediction. The hit list after the first iteration includes many hypothetical proteins annotated either as ATLS1-like light-inducible proteins or MIF-like proteins. But, starting from the second iteration, there are a growing number of hits to functionally characterized mammalian MIFs, including mouse and human MIF. The sequence of PmMIF is 34% identical with that of human MIF, and in the pairwise alignment there are no insertions or deletions (Figure 1B). We have selected PmMIF for further study in order to obtain insight into the structural and functional properties of this cyanobacterial MIF homologue.

Table 1: Kinetic Parameters for MIF, PmMIF, and PmMIF Mutants[a]

enzyme	substrate	k_{cat} (s^{-1})	K_m (μM)	k_{cat}/K_m (M^{-1} s^{-1})
MIF	**1**	114 ± 13	499 ± 116	2.3×10^5
MIF	**3**	147 ± 14	239 ± 57	6.2×10^5
PmMIF	**1**	0.31 ± 0.03	235 ± 61	1.3×10^3
PmMIF	**3**	0.05 ± 0.004	93 ± 28	5.4×10^2
P1A-PmMIF	**1**	0.01 ± 0.002	96 ± 55	1.0×10^2
E60C-PmMIF	**1**	1.27 ± 0.13	229 ± 57	5.5×10^3
E60S-PmMIF	**1**	2.44 ± 0.33	399 ± 111	6.1×10^3
G97N-PmMIF	**1**	0.24 ± 0.02	479 ± 76	5.0×10^2
W106V-PmMIF	**1**	0.57 ± 0.06	238 ± 66	2.4×10^3

[a]The steady-state kinetic parameters were determined at 22 °C in 20 mM NaH_2PO_4 buffer, pH 6.5. Errors are standard deviations from each fit.

Expression and Purification of PmMIF. The gene coding for PmMIF was amplified from genomic DNA of *P. marinus* strain MIT9313 and cloned in the expression vector pET20b(+), resulting in the construct pET20b(PmMIF-His). The PmMIF gene in pET20b(PmMIF-His) is under transcriptional control of the T7 promoter, and the recombinant enzyme was produced constitutively in *E. coli* BL21(DE3) as a C-terminal hexahistidine fusion protein. The recombinant enzyme was purified by a one-step Ni-based immobilized metal affinity chromatography protocol, which typically provides ~20 mg of homogeneous enzyme per liter of culture. Analysis of the purified enzyme by electrospray ionization mass spectrometry revealed one major peak that corresponds to a mass of 13305 ± 1 Da. A comparison of this value to the calculated subunit mass (13437 Da) indicates that the initiating methionine is removed during posttranslational processing, resulting in a protein with an N-terminal proline.

Tautomerase Activity of PmMIF. It has previously been determined that MIF functions as a tautomerase and processes substrates such as phenylenolpyruvate (**1**) and (*p*-hydroxyphenyl)enolpyruvate (**3**) (*16*−*20*). These observations prompted us to examine whether PmMIF catalyzes the tautomerization of these compounds. The results show that PmMIF catalyzes a tautomerization reaction using **1** or **3**, although not as efficiently as MIF (Table 1). MIF catalyzes the conversion of **1** to **2** (Scheme 1) with a $k_{cat} = 114\ s^{-1}$ and a K_m of 499 μM, resulting in a k_{cat}/K_m of $2.3 \times 10^5\ M^{-1}\ s^{-1}$. In comparison to MIF, PmMIF shows a 377-fold decrease in k_{cat}, a 2.1-fold decrease in K_m, and a 177-fold decrease in k_{cat}/K_m. A comparison of the parameters measured for the conversion of **3** to **4** shows that the k_{cat}, K_m, and k_{cat}/K_m values for PmMIF are 2940-, 2.6-, and 1148-fold lower, respectively, than those for MIF.

The PmMIF-catalyzed tautomerization of **3** (i.e., the enol form) was also monitored by ^1H NMR spectroscopy to verify that the product of the reaction is **4** (i.e., the keto form). The spectrum recorded immediately after dissolving (*p*-hydroxyphenyl)pyruvate in acetate buffer revealed two doublets in the aromatic region (at 7.55−7.57 and 6.81−6.82 ppm) and a singlet representing an olefinic proton at 6.23 ppm, which is consistent

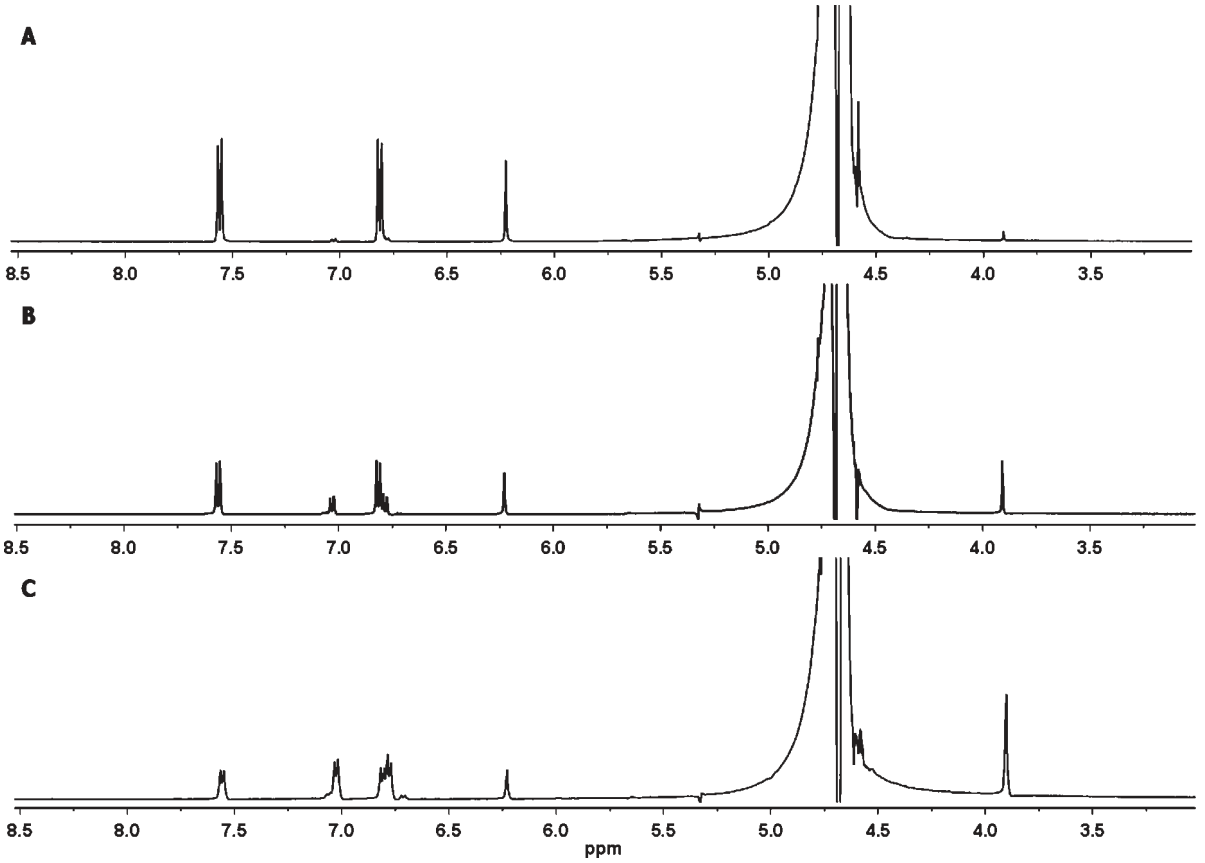

FIGURE 2: ^{1}H NMR spectra monitoring the conversion of (*p*-hydroxyphenyl)enolpyruvate (**3**) to (*p*-hydroxyphenyl)pyruvate (**4**). (A) Spectrum of unconverted **3**. (B) Spectrum of the nonenzymatic conversion of **3** to **4**. (C) Spectrum of the PmMIF-catalyzed conversion of **3** to **4**. The ^{1}H NMR signals for compounds **3** and **4** are described in the Experimental Procedures. Spectrum A was recorded immediately after dissolving **3** in acetate buffer, whereas spectra B and C were recorded after 30 min.

with the enol form (Figure 2A). The enzymatic conversion of the enol form yields the keto form, as indicated by changes in the chemical shifts of the aromatic protons (to 7.02−7.04 and 6.78−6.79 ppm) and the appearance of a singlet at 3.91 ppm, which corresponds to the methylene protons. After a 30 min incubation period, the ratio of keto:enol is ~2 (Figure 2C). For comparison, a 30 min incubation period in the absence of enzyme yields a keto:enol ratio of ~0.5 (Figure 2B). These observations confirm that PmMIF has low-level tautomerase activity and demonstrate that **4** is the product of the PmMIF-catalyzed conversion of **3**.

Since the N-terminal proline is expected to be important for the tautomerase activity of PmMIF (see below), we located the hexahistidine tag at the C-terminus of PmMIF. However, it remained possible that the hexahistidine tag could influence the tautomerase activity of PmMIF. To eliminate this concern, the native PmMIF protein without a fusion tag was also expressed and purified to homogeneity. Analysis of the kinetic properties of purified native PmMIF, using **1** as the substrate, yielded kinetic parameters (k_{cat} = 0.22 s^{-1}, K_m = 317 μM, and k_{cat}/K_m = 6.9 × 10^2 M^{-1} s^{-1}) very similar to those measured for the hexahistidine-tagged PmMIF. The sum of these observations shows that PmMIF has a tautomerase activity, but the activity is not as robust as that of MIF.

Inactivation of PmMIF by 3-Bromopyruvate. We investigated whether the tautomerase activity of PmMIF is sensitive to 3-bromopyruvate, an active site-directed irreversible inhibitor of MIF that covalently modifies the catalytic Pro-1 residue (*47*). After a 1 h incubation period (at 22 °C) with 3-bromopyruvate, the PmMIF sample had no residual tautomerase activity, whereas the MIF sample (which was used as a control) had ~5% residual activity. Incubation of PmMIF or MIF without inhibitor under the same conditions had no effect on activity. Gel filtration chromatography did not result in recovery of enzyme activity, indicative of covalent modification.

To confirm the covalent modification of PmMIF and MIF, the two protein samples were treated with 3-bromopyruvate, reduced by $NaBH_4$, and analyzed by ESI-MS. The observed monomer masses of modified PmMIF (13395 ± 3 Da) and modified MIF (13529 ± 3 Da) are in good agreement with the masses expected for the monomer labeled by a single lactyl group and reduced by $NaBH_4$ (13395 and 13527 Da, respectively) (*47*).[3] These results show that 3-bromopyruvate is responsible for the irreversible inhibition of both PmMIF and MIF and provide further evidence indicating that PmMIF is responsible for the observed tautomerase activity.

Kinetic Properties of the P1A Mutant of PmMIF. Kinetic, site-directed mutagenesis, NMR, and crystallographic analyses identified Pro-1 as the critical active site base for the tautomerase activity of MIF (*19*, *20*, *47*−*49*). To assess the importance of Pro-1 for the tautomerase activity of PmMIF, the P1A mutant was constructed, overproduced in *E. coli* BL21-(DE3), and purified to homogeneity using the immobilized metal affinity chromatography protocol developed for the wild-type

[3]We also observed that prolonged incubation of PmMIF and MIF at 22 °C (in the presence of 3-bromopyruvate) gives multiple labeling events per monomer, which may result from the partial denaturation of the proteins under these conditions.

enzyme. The kinetic properties of the P1A mutant were analyzed using **1** as the substrate. The P1A mutant showed a 30-fold decrease in k_{cat} and a 2.4-fold decrease in K_m, resulting in a 13-fold decrease in k_{cat}/K_m (Table 1). These results provide additional evidence indicating that PmMIF is responsible for the observed activities and that Pro-1 is critical for activity.

Oxidoreductase Activity of PmMIF. It has previously been reported that MIF functions as an oxidoreductase and reduces small molecule disulfides such as 2-hydroxyethyl disulfide (HED) (*25*, *26*). This activity is based on a thioredoxin-like Cys-X-X-Cys motif (Figure 1B). We investigated whether PmMIF (with and without hexahistidine tag) can catalyze the reduction of HED. The results show that PmMIF does not reduce this disulfide. This is not surprising in view of the lack of the Cys-X-X-Cys motif in PmMIF (Figure 1B) and the very low level reductase activity of MIF (which was used as a control).

We next investigated whether the introduction of a Cys-X-X-Cys motif into PmMIF would give the enzyme the ability to reduce HED. The motif was introduced by constructing two different mutants: the single mutant E60C and the quadruple mutant T56C/C57A/Y58L/V59C. In the latter mutant, the motif is identical and in the same position in the alignment as that of MIF, whereas in the single mutant the Cys-X-X-Cys motif is shifted by one amino acid position (Figure 1B). In addition, we have mutated Glu-60 to the corresponding residue in MIF, yielding the E60S mutant. The three mutants were overproduced in *E. coli* BL21(DE3), purified to homogeneity, and assayed for their ability to reduce HED. As observed with wild-type PmMIF, the mutants did not exhibit detectable reductase activity.

The kinetic properties of the three mutants were also analyzed using **1** as the substrate. Replacement of Glu-60 with a cysteine or serine resulted in active enzymes with a surprisingly improved phenylpyruvate tautomerase activity (Table 1). The major effect of these mutations is observed in k_{cat}; there is a 4- and 8-fold increase in the k_{cat} values for the E60C and E60S mutants, respectively. Analysis of the kinetic properties of the quadruple mutant yielded kinetic parameters very similar to those measured for wild-type PmMIF (not shown).

Crystal Structure of PmMIF. To enhance our understanding of the relationship between PmMIF and mammalian MIFs, we have determined the X-ray crystal structure of PmMIF at 1.63 Å resolution. The crystallographic *R*-factor for the final model was 16.4% (R_{free} of 21.3%) (Table 2). PmMIF adopts a trimeric ring architecture similar to the other known MIF structures with each monomer composed of a four-stranded mixed β-sheet and two antiparallel α-helices stacked against the β-sheet on the outside of the trimer (Figure 3A). In the trimeric arrangement, the four-stranded β-sheet of each subunit is extended by two small β-strands contributed from the adjacent subunits. The overall trimer structure of PmMIF is highly similar to that of the mammalian MIFs. A least-squares fit using C_α atoms from all three chains in the PmMIF trimer gives rmsd values of 0.83 and 0.95 Å against the structures of mouse MIF (PDB entry 1MFF) (*20*) and human MIF (PDB entry 1MIF) (*22*), respectively.

Tautomerase Active Site of PmMIF. To define the structural basis for the tautomerase activity of PmMIF, cocrystallization experiments with substrates **1** and **3** (and their keto isomers) (Scheme 1) were attempted. Although well-diffracting crystals were obtained at similar crystallization conditions as before, the derived electron density revealed no bound substrate in the active site. Hence, these cocrystallization experiments were unsuccessful. However, inspection of the $2F_o - F_c$ and $F_o - F_c$ difference Fourier maps revealed additional electron density near Pro-1 in all analyzed crystallographic data sets (from crystals grown in either the absence or presence of substrate), indicating the presence of a bound ligand. This electron density may be interpreted as a diethylene glycol molecule, small amounts of which are present in the crystallization precipitant PEG300 (up to 0.4% according to the manufacturer), or, alternatively, as the

Table 2: Crystallographic Data and Refinement Statistics

data collection	
space group	$P6_3$
unit cell dimensions (Å)	$a = b = 52.5$; $c = 64.0$
resolution range (Å)	26.2−1.63
no. of total measurements	68425
no. of unique reflections	12309
R_{sym} (%)	7.4 (26.1)
completeness (%)	98.7 (91.3)
average I/σ	15.3 (6.4)
refinement	
contents of AU	
protein	1 chain, residues 1−114
waters	114
other	1 diethylene glycol
R/R_{free}	16.4/21.3
geometry	
rmsd bonds (Å)	0.010
rmsd angles (deg)	1.2
Ramachandran plot (%) (favored/allowed)	99.1/0.9

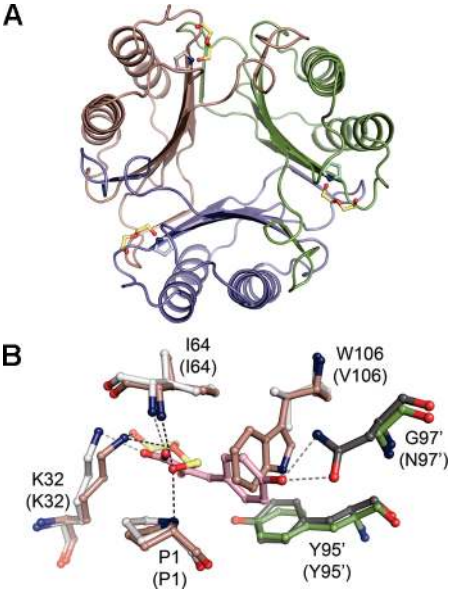

FIGURE 3: Crystal structure of PmMIF. (A) Ribbon diagram of the homotrimeric structure of PmMIF. For clarity, each subunit is shown in a different color (blue, green, and brown). The catalytic Pro-1 and the bound diethylene glycol molecule (or PEG terminus) are shown in ball-and-stick representation. (B) An overlay of the active sites of PmMIF complexed with diethylene glycol and human MIF complexed with (*p*-hydroxyphenyl)enolpyruvate (*48*). The active site residues are shown in ball-and-stick representation, and the atoms are colored as follows: red, oxygens; blue, nitrogens; brown and green, carbons of PmMIF; white and gray, carbons of human MIF; yellow, carbons of diethylene glycol; pink, carbons of (*p*-hydroxyphenyl)enolpyruvate. The roles of the key active site residues of human MIF (residue labels shown in parentheses) and their interactions are discussed in the text. The prime designation indicates that Y95 and G97 (N97 in human MIF) come from an adjacent monomer. Broken lines in black and gray indicate the observed protein−ligand hydrogen bonds in the structures of PmMIF and human MIF, respectively.

terminal units of a polyethylene glycol (PEG) molecule that protrudes into the active site, with its remainder being invisible due to disorder. The presumed diethylene glycol molecule or PEG terminus forms hydrogen-bonding interactions with Pro-1, Lys-32, and Ile-64 at the mouth of the putative active site cavity (Figure 3B).

To better define the tautomerase active site of PmMIF, we superimposed the structures of the active site regions of PmMIF and human MIF in complex with (*p*-hydroxyphenyl)enolpyruvate (**3**, Scheme 1) (Figure 3B). The structure of human MIF complexed with **3** (*48*) has identified the tautomerase active site and provided the essential structural information for the identification of the substrate interactions within the human MIF−substrate complex. In this complex, the catalytically important Pro-1 forms a hydrogen bond with C-3 of **3**, Lys-32 and Ile-64 form hydrogen-bonding interactions with the carboxylate group, Asn-97 forms hydrogen bonds with the phenolic hydroxyl group, and Tyr-95 and Val-106 interact with the phenyl group of **3**. Interestingly, four of the six active site residues that are interacting with the substrate (Pro-1, Lys-32, Ile-64, and Tyr-95) are conserved in PmMIF, both in sequence and in position. However, two residues, Asn-97 and Val-106, are not conserved and replaced by Gly-97 and Trp-106 in PmMIF (Figure 3B). The replacement of Asn-97 in human MIF by Gly-97 in PmMIF eliminates two side chain hydrogen bonds with substrate, assuming that substrate binds in the same orientation in the active site of PmMIF as compared to human MIF. The replacement of Val-106 in human MIF by the larger residue Trp-106 in PmMIF is potentially even more significant because Trp-106 partially fills the volume that is occupied by the phenyl group of the substrate in the human MIF−substrate complex (Figure 3B) (*48*). This suggests either that substrate has a different binding mode in PmMIF compared to human MIF, preventing a clash with Trp-106, or that conformational changes take place in PmMIF upon substrate binding, repositioning Trp-106 and generating the catalytically active state.

Structure-Based Mutagenesis Studies of PmMIF. The preceding comparison of the crystal structures of PmMIF and human MIF uncovered two unique active site residues in PmMIF, Gly-97 and Trp-106, that may contribute to its decreased tautomerase activity compared to human MIF. To investigate this possibility, these two active site residues in PmMIF have been mutated to the positionally conserved ones in human MIF. The two mutants (G97N and W106V) were overproduced in *E. coli* BL21(DE3), purified to homogeneity, and assayed for their ability to convert **1** to **2**. For the G97N mutant there is only an ~2-fold increase in K_m, whereas for the W106V mutant there is, at best, only a 2-fold increase in k_{cat} (Table 1). These results suggest that the replacement of Asn-97 and Val-106 in human MIF by Gly-97 and Trp-106 in PmMIF appears not to be responsible for the observed low-level activity of PmMIF.

DISCUSSION

We report herein the discovery and characterization of a cyanobacterial protein, designated PmMIF, that shares significant structural and functional similarities with the mammalian cytokine MIF. While several MIF homologues have been identified in eukaryotic parasites (*27*−*35*), where they are thought to play a role in modulating the host immune response, PmMIF is the first nonparasitic, bacterial MIF-like protein characterized in detail. Like eukaryotic MIFs, PmMIF is an active tautomerase, converting the substrates phenylenolpyruvate (**1**) and (*p*-hydroxyphenyl)enolpyruvate (**3**). The tautomerase activity levels are similar to those of MIF-like proteins from eukaryotic parasites, but much lower than those of human and mouse MIF.[4] In contrast to several eukaryotic MIFs, however, PmMIF does not exhibit oxidoreductase activity.

The MIF family is one of the major families within the tautomerase superfamily, a group of structurally homologous proteins that are characterized by a $\beta-\alpha-\beta$ building block and a catalytic amino-terminal proline (Pro-1) (*23*, *24*). Elucidation of the crystal structure of PmMIF (to 1.63 Å resolution) established that this cyanobacterial protein has the same overall $\beta-\alpha-\beta$ structural fold as previously characterized eukaryotic members of the MIF family. The importance of the conserved Pro-1 in catalysis was demonstrated by site-directed mutagenesis of PmMIF: the replacement of Pro-1 with an alanine resulted in an enzyme with strongly reduced tautomerase activity. Furthermore, reaction of PmMIF with 3-bromopyruvate, an active site-directed irreversible inhibitor of MIF that covalently modifies its catalytic Pro-1 residue (*47*), led to the alkylation of PmMIF and the concomitant loss of catalytic activity. The shared sequence identity and tautomerase activities and the conservation of the overall structural fold and catalytic Pro-1 residue firmly link PmMIF to the MIF family within the tautomerase superfamily. On the basis of these observations, we propose that PmMIF is part of the subfamily of bacterial $\beta-\alpha-\beta$-fold proteins from which eukaryotic MIFs may have originated.

Although the overall trimeric structures are very similar, the putative active site region of PmMIF shows distinctive features from that of human and mouse MIF. Structural comparisons showed that four of the six active site residues implicated in substrate binding and/or catalysis in human MIF (Pro-1, Lys-32, Ile-64, and Tyr-95) are conserved in PmMIF (Figure 3B). However, two substrate-binding residues in human MIF, Asn-97 and Val-106, are replaced by Gly-97 and Trp-106 in PmMIF. These active site differences may reflect the different substrate specificities of cyanobacterial and human MIF, given that the physiological substrate of PmMIF has yet to be identified (see below). Notably, Trp-106 is fully conserved in the identified cyanobacterial MIF homologues, whereas the amino acid at position 97 is semiconserved, being either a glycine, glutamate, or asparagine (Figure 1A).

Surprisingly, mutation of Gly-97 and Trp-106 in PmMIF to their respective counterparts in human MIF had no significant influence on the level of phenylpyruvate tautomerase activity. This is quite remarkable given the fact that Trp-106, instead of the shorter Val-106, partially fills the volume that is occupied by the phenyl group of the substrate in the human MIF−substrate complex (Figure 3B) (*48*). One potential explanation for these observations is that conformational changes take place in PmMIF upon substrate binding, repositioning Trp-106 and thereby generating the catalytically active state of the enzyme. The notion that Trp-106 may occlude the binding pocket for

[4]The rate for the spontaneous nonenzymatic ketonization of **1** has not been reported. However, the rate for the uncatalyzed ketonization of enolpyruvate in phosphate buffer in D_2O ($\sim 2.0 \times 10^{-3}$ s^{-1}) has been determined (*50*). Using this value and the k_{cat} value for the PmMIF-catalyzed ketonization of **1** (Table 1), it can be roughly estimated that PmMIF affords a 150-fold rate enhancement. The actual rate enhancement might be somewhat different because **1** is more stable than enolpyruvate and because the ketonization of enolpyruvate in aqueous buffer will likely be severalfold faster than the reported rate in buffer in D_2O.

aromatic substrates also prompted us to investigate whether alternative nonaromatic pyruvate derivatives may be processed by PmMIF. We have tested acetoacetate, oxaloacetate, and 2-hydroxymuconate as potential substrates for PmMIF, but no detectable tautomerase activity was observed. Work is in progress to explore additional pyruvate derivatives as possible substrates for PmMIF.[5]

Another potential explanation for the lack of a significant kinetic effect of the W106V mutation is that the aromatic substrate has a different binding mode in PmMIF compared to human MIF. Support for this view comes from the interactions observed in the recently solved crystal structure of *Plasmodium yoelii* MIF (PyMIF) complexed with (*p*-hydroxyphenyl)pyruvate (**4**) (*51*). In the structure of the PyMIF−substrate complex, the substrate is bound in an orientation different from that observed in the structure of the human MIF−substrate complex. The change in the binding orientation in PyMIF prevents a clash between the substrate's phenyl group and the large phenylalanine residue found at position 106. It has been postulated that this different substrate binding mode also accounts for the lower level of phenylpyruvate tautomerase activity of PyMIF (*51*).

Taken together, these observations implicate factors beyond the core set of six active site residues in MIF catalysis and substrate specificity. Hence, in-depth mechanistic, structural, and mutational studies of PmMIF are needed to identify the additional features necessary for a fully active phenylpyruvate tautomerase. In this context, it is important to emphasize that the PmMIF mutants E60C and E60S have surprisingly increased tautomerase activity levels (4- and 8-fold, respectively). Residue Glu-60 is located at the monomer−monomer interface within the trimer, quite far from the tautomerase active site, and the exact mechanism of the kinetic effects of the E60C and E60S mutations is unknown. Nonetheless, these findings suggest that the lower level of tautomerase activity of PmMIF may be the result of a combination of effects, including the suboptimal positioning of the substrate.

To obtain a better understanding of the catalytic mechanism of PmMF, it would be highly desirable to have a crystal structure of PmMIF complexed with substrate at the active site. However, our attempts to crystallize PmMIF in complex with substrate **1** or **3** (or their keto isomers) using cocrystallization experiments have been unsuccessful so far. Our failure to obtain such a crystal structure could be due to a number of factors. We have considered the possibility that diethylene glycol, which is indicated as a possible ligand bound in the active site of PmMIF (Figure 3), could act as a competitive inhibitor and prevent substrate from binding. Hence, we have tested diethylene glycol as a potential inhibitor of PmMIF. In the presence of **1** (at 300 μM), the enzyme was only slightly inhibited (~15%) by 10 mM diethylene glycol. As the concentration of diethylene glycol in the crystallization solution is estimated to be ≤10 mM, we concluded that the possibility that diethylene glycol prevents substrate from binding is not very likely. Additional experiments are underway to obtain a structure of the enzyme−substrate complex, including soaking experiments and cocrystallization efforts using different crystallization conditions (in the absence of PEG).

In summary, the discovery of a new subgroup of cyanobacterial proteins in the MIF family, along with the structural and functional characterization of PmMIF, demonstrates that MIF-like proteins have a widespread distribution and are found not only in eukaryotic parasites but also in free-living bacteria. This invites speculation about the intrinsic physiological function of these MIF-like proteins. One important fundamental question concerns whether PmMIF exhibits immunostimulatory features similar to those of mammalian MIFs and MIF-like proteins found in parasitic nematodes and protozoa (*27*−*34*). In order to address this question, it will be necessary to test whether PmMIF can influence the functional responses of human immune cells and shows significant binding interaction with the human MIF receptor, CD74 (*11*, *12*). Such efforts are being pursued in our laboratories and may help to establish whether parasitic MIF-like proteins could function as "accidental" effector molecules of the human immune response.

[5]The possibility that PmMIF has other activities in addition to its tautomerase activity cannot be excluded. Also note that the biological relevance of MIF's tautomerase activities is unknown.

ACKNOWLEDGMENT

We thank Dr. S. W. Chisholm (Massachusetts Institute of Technology, Cambridge, MA) for the kind gift of genomic DNA of *P. marinus* strain MIT9313 and Dr. C. P. Whitman (University of Texas at Austin, TX) for the kind gift of plasmid pET11b-(MIF).

REFERENCES

1. Bloom, B. R., and Bennett, B. (1966) Mechanism of a reaction *in vitro* associated with delayed-type hypersensitivity. *Science 153*, 80–82.
2. David, J. R. (1966) Delayed hypersensitivity *in vitro*: its mediation by cell-free substances formed by lymphoid cell-antigen interaction. *Proc. Natl. Acad. Sci. U.S.A. 56*, 72–77.
3. Lue, H., Kleemann, R., Calandra, T., Roger, T., and Bernhagen, J. (2002) Macrophage migration inhibitory factor (MIF): mechanisms of action and role in disease. *Microbes Infect. 4*, 449–460.
4. Bucala, R. (2000) A most interesting factor. *Nature 408*, 146–147.
5. Bernhagen, J., Mitchell, R. A., Calandra, T., Voelter, W., Cerami, A., and Bucala, R. (1994) Purification, bioactivity, and secondary structure analysis of mouse and human macrophage migration inhibitory factor (MIF). *Biochemistry 33*, 14144–14155.
6. Donnelly, S. C., Haslett, C., Reid, P. T., Grant, I. S., Wallace, W. A. H., Metz, C. N., Bruce, L. J., and Bucala, R. (1997) Regulatory role for macrophage migration inhibitory factor in acute respiratory distress syndrome. *Nat. Med. 3*, 320–323.
7. Mikulowska, A., Metz, C. N., Bucala, R., and Holmdahl, R. (1997) Macrophage migration inhibitory factor is involved in the pathogenesis of collagen type II-induced arthritis in mice. *J. Immunol. 158*, 5514–5517.
8. Morand, E. F., Leech, M., and Bernhagen, J. (2006) MIF: a new cytokine link between rheumatoid arthritis and atherosclerosis. *Nat. Rev. Drug Discovery 5*, 399–410.
9. Calandra, T, and Roger, T. (2003) Macrophage migration inhibitory factor: a regulator of innate immunity. *Nat. Rev. Immunol. 3*, 791–800.
10. Calandra, T., Bernhagen, J., Metz, C. N., Spiegel, L. A., Bacher, M., Donnelly, T., Cerami, A., and Bucala, R. (1995) MIF as a glucocorticoid-induced modulator of cytokine production. *Nature 377*, 68–71.
11. Leng, L., Metz, C. N., Fang, Y., Xu, J., Donnelly, S., Baugh, J., Delohery, T., Chen, Y., Mitchell, R. A., and Bucala, R. (2003) MIF signal transduction initiated by binding to CD74. *J. Exp. Med. 197*, 1467–1476.
12. Leng, L., and Bucala, R. (2006) Insight into the biology of macrophage migration inhibitory factor (MIF) revealed by the cloning of its cell surface receptor. *Cell Res. 16*, 162–168.
13. Shi, X., Leng, L., Wang, T., Wang, W., Du, X., Li, J., McDonald, C., Chen, Z., Murphy, J. W., Lolis, E., Noble, P., Knudson, W., and Bucala, R. (2006) CD44 is the signalling component of the macrophage migration inhibitory factor-CD74 receptor complex. *Immunity 25*, 595–606.
14. Bernhagen, J., Krohn, R., Lue, H., Gregory, J. L., Zernecke, A., Koenen, R. R., Dewor, M., Georgiev, I., Schober, A., Leng, L., Kooistra, T., Fingerle-Rowson, G., Ghezzi, P., Kleemann, R., McColl, S. R., Bucala, R., Hickey, M. J., and Weber, C. (2007) MIF is a noncognate ligand of CXC chemokine receptors in inflammatory and atherogenic cell recruitment. *Nat. Med. 13*, 587–596.

15. Schwartz, V., Lue, H., Kraemer, S., Korbiel, J., Krohn, R., Ohl, K., Bucala, R., Weber, C., and Bernhagen, J. (2009) A functional heteromeric MIF receptor formed by CD74 and CXCR4. *FEBS Lett. 583*, 2749–2757.
16. Rosengren, E., Bucala, R., Aman, P., Jacobsson, L., Odh, G., Metz, C. N., and Rorsman, H. (1996) The immunoregulatory mediator macrophage migration inhibitory factor (MIF) catalyzes a tautomerization reaction. *Mol. Med. 2*, 143–149.
17. Rosengren, E., Aman, P., Thelin, S., Hansson, C., Ahlfors, S., Bjork, P., Jacobsson, L., and Rorsman, H. (1997) The macrophage migration inhibitory factor (MIF) is a phenylpyruvate tautomerase. *FEBS Lett. 417*, 85–88.
18. Rosengren, E., Thelin, S., Aman, P., Hansson, C., Jacobsson, L., and Rorsman, H. (1997) The protein catalyzing the conversion of D-dopachrome to 5,6-dihydroxyindole is a phenylpyruvate tautomerase. *Melanoma Res. 7*, 1–2.
19. Bendrat, K., Al-Abed, Y., Callaway, D. J., E., Peng, T., Calandra, T., Metz, C. N., and Bucala, R. (1997) Biochemical and mutational investigations of the enzymatic activity of macrophage migration inhibitory factor. *Biochemistry 36*, 15356–15362.
20. Stamps, S. L., Taylor, A. B., Wang, S. C., Hackert, M. L., and Whitman, C. P. (2000) Mechanism of the phenylpyruvate tautomerase activity of macrophage migration inhibitory factor: properties of the P1G, P1A, Y95F, and N97A mutants. *Biochemistry 39*, 9671–9678.
21. Suzuki, M., Sugimoto, H., Nakagawa, A., Tanaka, I., Nishihira, J., and Sakai, M. (1996) Crystal structure of the macrophage migration inhibitory factor from rat liver. *Nat. Struct. Biol. 3*, 259–266.
22. Sun, H.-W., Bernhagen, J., Bucala, R., and Lolis, E. (1996) Crystal structure at 2.6 Å resolution of human macrophage migration inhibitory factor. *Proc. Natl. Acad. Sci. U.S.A. 93*, 5191–5196.
23. Murzin, A. G. (1996) Structural classification of proteins: new superfamilies. *Curr. Opin. Struct. Biol. 6*, 386–394.
24. Poelarends, G. J., Puthan Veetil, V., and Whitman, C. P. (2008) The chemical versatility of the β-α-β fold: catalytic promiscuity and divergent evolution in the tautomerase superfamily. *Cell. Mol. Life Sci. 65*, 3606–3618.
25. Kleemann, R., Kapurniotu, A., Frank, R. W., Gessner, A., Mischke, R., Flieger, O., Juttner, S., Brunner, H., and Bernhagen, J. (1998) Disulfide analysis reveals a role for macrophage migration inhibitory factor (MIF) as thiol-protein oxidoreductase. *J. Mol. Biol. 280*, 85–102.
26. Nguyen, M. T., Beck, J., Lue, H., Fünfzig, H., Kleemann, R., Koolwijk, P., Kapurniotu, A., and Bernhagen, J. (2003) A 16-residue peptide fragment of macrophage migration inhibitory factor, MIF-(50−65), exhibits redox activity and has MIF-like biological functions. *J. Biol. Chem. 278*, 33654–33671.
27. Pastrana, D. V., Raghavan, N., FitzGerald, P., Eisinger, S. W., Metz, C., Bucala, R., Schleimer, R. P., Bickel, C., and Scott, A. L. (1998) Filarial nematode parasites secrete a homologue of the human cytokine macrophage migration inhibitory factor. *Infect. Immun. 66*, 5955–5963.
28. Wu, Z., Boonmars, T., Nagano, I., Nakada, T., and Takahashi, Y. (2003) Molecular expression and characterization of a homologue of host cytokine macrophage migration inhibitory factor from *Trichinella* spp. *J. Parasitol. 89*, 507–515.
29. Falcone, F. H., Loke, P., Zang, X., MacDonald, A. S., Maizels, R. M., and Allen, J. E. (2001) A *Brugia malayi* homolog of macrophage migration inhibitory factor reveals an important link between macrophages and eosinophil recruitment during nematode infection. *J. Immunol. 167*, 5348–5354.
30. Zang, X., Taylor, P., Wang, J. M., Meyer, D. J., Scott, A. L., Walkinshaw, M. D., and Maizels, R. M. (2002) Homologues of human macrophage migration inhibitory factor from a parasitic nematode. Gene cloning, protein activity, and crystal structure. *J. Biol. Chem. 277*, 44261–44267.
31. Cho, Y., Jones, B. F., Vermeire, J. J., Leng, L., Difedele, L., Harrison, L. M., Xiong, H., Kwong, Y. K., Chen, Y., Bucala, R., Lolis, E., and Cappello, M. (2007) Structural and functional characterization of a secreted hookworm macrophage migration inhibitory factor (MIF) that interacts with the human MIF receptor CD74. *J. Biol. Chem. 282*, 23447–23456.
32. Augustijn, K. D., Kleemann, R., Thompson, J., Kooistra, T., Crawford, C. E., Reece, S. E., Pain, A., Siebum, A. H., Janse, C. J., and Waters, A. P. (2007) Functional characterization of the *Plasmodium falciparum* and *P. berghei* homologues of macrophage migration inhibitory factor. *Infect. Immun. 75*, 1116–1128.
33. Cordery, D. V., Kishore, U., Kyes, S., Shafi, M. J., Watkins, K. R., Williams, T. N., Marsh, K., and Urban, B. C. (2007) Characterization of a *Plasmodium falciparum* macrophage-migration inhibitory factor homologue. *J. Infect. Dis. 195*, 905–912.
34. Kamir, D., Zierow, S., Leng, L., Cho, Y., Diaz, Y., Griffith, J., McDonald, C., Merk, M., Mitchell, R. A., Trent, J., Chen, Y., Kwong, Y-K. A., Xiong, H., Vermeire, J., Capello, M., McMahon-Pratt, D., Walker, J., Bernhagen, J., Lolis, E., and Bucala, R. (2008) A *Leishmania* ortholog of macrophage migration inhibitory factor modulates host macrophage responses. *J. Immunol. 180*, 8250–8261.
35. Hoerauf, A., Satoguina, J., Saeftel, M., and Specht, S. (2005) Immunomodulation by filarial nematodes. *Parasite Immunol. 27*, 417–429.
36. Sambrook, J., Fritsch, E. F., and Maniatis, T. (1989) Molecular Cloning: A Laboratory Manual, 2nd ed., Cold Spring Harbor Laboratory, Cold Spring Harbor, NY.
37. Waddell, W. J. (1956) A simple ultraviolet spectrophotometric method for the determination of protein. *J. Lab. Clin. Med. 48*, 311–314.
38. Rocap, G., Larimer, F. W., Lamerdin, J., Malfatti, S., Chain, P., Ahlgren, N. A., Arellano, A., Coleman, M., Hauser, L., Hess, W. R., Johnson, Z. I., Land, M., Lindell, D., Post, A. F., Regala, W., Shah, M., Shaw, S. L., Steglich, C., Sullivan, M. B., Ting, C. S., Tolonen, A., Webb, E. A., Zinser, E. R., and Chisholm, S. W. (2003) Genome divergence in two *Prochlorococcus* ecotypes reflects oceanic niche differentiation. *Nature 424*, 1042–1047.
39. Ho, S. N., Hunt, H. D., Horton, R. M., Pullen, J. K., and Pease, L. R. (1989) Site-directed mutagenesis by overlap extension using the polymerase chain reaction. *Gene 77*, 51–59.
40. Wang, S. C., Johnson, W. H., Jr., Czerwinski, R. M., Stamps, S. L., and Whitman, C. P. (2007) Kinetic and stereochemical analysis of YwhB, a 4-oxalocrotonate tautomerase homologue in *Bacillus subtilis*: mechanistic implications for the YwhB- and 4-oxalocrotonate tautomerase-catalyzed reactions. *Biochemistry 23*, 11919–11929.
41. Leslie, A. G. (2006) The integration of macromolecular diffraction data. *Acta Crystallogr., Sect. D: Biol. Crystallogr. 62*, 48–57.
42. McCoy, A. J. (2007) Solving structures of protein complexes by molecular replacement with Phaser. *Acta Crystallogr., Sect. D: Biol. Crystallogr. 63*, 32–41.
43. Morris, R. J., Perrakis, A., and Lamzin, V. S. (2003) ARP/wARP and automatic interpretation of protein electron density maps. *Methods Enzymol. 374*, 229–244.
44. Emsley, P., and Cowtan, K. (2004) Coot: model-building tools for molecular graphics. *Acta Crystallogr., Sect. D: Biol. Crystallogr. 60*, 2126–2132.
45. Murshudov, G. N., Vagin, A. A., and Dodson, E. J. (1997) Refinement of macromolecular structures by the maximum-likelihood method. *Acta Crystallogr., Sect. D: Biol. Crystallogr. 53*, 240–255.
46. Davis, I. W., Leaver-Fay, A., Chen, V. B., Block, J. N., Kapral, G. J., Wang, X., Murray, L. W., Arendall, W. B., III, Snoeyink, J., Richardson, J. S., and Richardson, D. C. (2007) MolProbity: all-atom contacts and structure validation for proteins and nucleic acids. *Nucleic Acids Res. 35*, W375–383.
47. Stamps, S. L., Fitzgerald, M. C., and Whitman, C. P. (1998) Characterization of the role of the amino-terminal proline in the enzymatic activity catalyzed by macrophage migration inhibitory factor. *Biochemistry 37*, 10195–10202.
48. Lubetsky, J. B., Swope, M., Dealwis, C., Blake, P., and Lolis, E. (1999) Pro-1 of macrophage migration inhibitory factor functions as a catalytic base in the phenylpyruvate tautomerase activity. *Biochemistry 38*, 7346–7354.
49. Taylor, A. B., Johnson, W. H., Jr., Czerwinski, R. M., Li, H.-S., Hackert, M. L., and Whitman, C. P. (1999) Crystal structure of macrophage migration inhibitory factor complexed with (*E*)-2-fluoro-*p*-hydroxycinnamate at 1.8 Å resolution: implications for enzymatic catalysis and inhibition. *Biochemistry 38*, 7444–7452.
50. Peliska, J. A., and O'Leary, M. H. (1991) Preparation and properties of enolpyruvate. *J. Am. Chem. Soc. 113*, 1841–1842.
51. Shao, D., Zhong, X., Zhou, Y.-F., Han, Z., Lin, Y., Wang, Z., Bu, L., Zhang, L., Su, X.-D., and Wang, H. (2010) Structural and functional comparison of MIF ortholog from *Plasmodium yoelii* with MIF from its rodent host. *Mol. Immunol. 47*, 726–737.